RC LACE research stay report

Topic: Mixing length computation in TOUCANS

Executed by: Mario Hrastinski

Supported by: Ján Mašek and Radmila Brožková

Prague, 14th May – 8th June 2018

1. Introduction

This stay continues the work performed during two previous stays at Czech Hydrometeorological Institute (CHMI)[1,2], which is related to the part of the ***APLPAR*** subroutine code in-between two calls of the ***ACMIXELEN*** subroutine. The focus is on development and testing of TKE-based mixing length formulations within TOUCANS (Third Order moments Unified Condesation Accounting and N-dependent Solver for turbulence and diffusion) turbulence parametrization of the ALARO-1 physics package, with emphasis on the Bougeault and Lacarrere (1989)[3] formulation (BL89). Theoretical background of the mixing length in TOUCANS and BL89 method are covered in previous reports[1,2], so here we will (with few exceptions) only refer to corresponding equations from there.

2. Work and results

2.1. Code phasing and reorganization

The code version which performs stability-dependent (SD) conversion from TKE-based mixing length formulations (L_{TKE}) to Prandtl type mixing length (l_m) is phased from CY38t1tr-op4 to CY38t1trlx-op8 branch of the ALADIN-CZ configuration of the ALADIN system. With transition from modified Richardson gradient number (Ri_g) shallow convection (SC) scheme (*LCOEFK_RIS=.TRUE.*) to mass-flux SC approach (*LCOEFK_MSC=.TRUE.*), and by moving the moist gustiness correction computation (MGCC) from ***ACMRIP*** to ***ACMIXELEN*** subroutine (where it is applied), the code is reduced to a single call of ***ACMIXELEN***. Unlike previously (last year's stay) when we were compelled to dry SD computation in the first call of ***ACMIXELEN*** (to

produce mixing length for MGCC and moist anti-fibrillation of modified Ri_g) and then used moist stability functions (computed in-between two calls) in the second call of ***ACMIXELEN***, here we achieve full moist treatment of SD conversion coefficient (SDCC)[1] (eq. (2) and (7) below). During this part of the code reorganization one bug was found and corrected (double counting of moist effects in computation of mean temperature between two adjacent model levels).

2.2. Mixing length experiments and theoretical background

By default it is assumed in TOUCANS that $L=L_{TKE}=L_{BL89}$, which is given by:

$$L=\left(L_K^3\cdot L_\epsilon\right)^{1/4}=\frac{C_\epsilon}{\nu^3}\cdot l_m \tag{1}$$

where L_K and L_ε are length scales for exchange processes and dissipation of turbulence (check for their definitions below; eq. (2) and (7)), while C_ε and ν are constants controlling the intensity of turbulence dissipation and overall intensity of turbulence. As default assumption led to underestimation of mixing in the PBL and generally poor scores[1],[2],[4], we decided to move the focus towards two other TKE-based scales available in the code, i.e. L_K and L_ε. For this reason, here we start with assumption that $L_{TKE}=L_{BL89}$ is proportional to L_K, which is given by:

$$L_K=\frac{C_\epsilon}{\nu^3}\cdot\frac{f\left(Ri_g\right)^{1/4}}{\chi_3^{1/2}}\cdot l_m \tag{2}$$

where $f(Ri_g)$ is function of Ri_g and χ_3 is stability function for momentum. Notice that both (1) and (2) don't ensure matching of l_m with similarity laws in the surface layer due to $C_\varepsilon/\nu \approx 6$ (not even at neutrality; $C_\varepsilon=0.871$ and $\nu=0.526$ for model II). To achieve this for SDCC approach we need to choose: i) L_K-L_{TKE} proportionality constant and ii) an averaging operator for L_{up} and L_{down}. First we choose the proportionality constant:

$$L_K=\frac{C_\epsilon}{\nu^3\cdot\kappa}\cdot L_{TKE} \tag{3}$$

where κ is von Karman constant. By merging (2) and (3) we get:

$$l_m=\kappa\cdot\frac{\chi_3^{1/2}}{f\left(Ri_g\right)^{1/4}}\cdot L_{TKE} \tag{4}$$

1 Stability-dependend (SD) conversion coefficient (SDCC) is a factor containing the ratio of $f(Ri_g)$ and χ_3, e.g. eq. (2), (4) and (7). Notice that it doesn't include constants C_ε and ν.

It still remains to choose an averaging operator for vertical displacement of air parcel in adiabatic process. The following two operators are selected for testing here:

$$L_{TKE}=min\left(L_{up},L_{down}\right) \tag{5a}$$

$$L_{TKE}=min\left(z,\sqrt{L_{up}\cdot L_{down}}\right) \tag{5b}$$

where z is height of the starting model level and also a limit for downwards displacement. As it is seen on Fig 1., SDCC for L_K is ≈ 1 near neutrality. This ensures matching of l_m with similarity theory, if proportionality constant (eq. (3)) and averaging operator (eq. (5a-5b)) are properly selected. Farther from neutrality, SDCC is expected to produce additional variability of l_m and related prognostic parameters.

Testing is performed for two cases: i) summer convection case (28-30.6.2017.) and ii) winter case (15-17.1.2017.). However, with single exception, here we will present only the results for the first one. During initial tests a problem with segmentation fault appeared. It turned out that it is related to the way how $f(Ri_g)$ is calculated (check eq. (94) in [4] or eq. (3) in [2]), i. e. protection of Ri_g against division by zero in computation of stability functions (eq. (14)-(16) in [4]) leads to $f(Ri_g)$ and mixing length being negative at times, which causes model execution to fail after several time steps. An alternative equation for $f(Ri_g)$, which always gives positive values, is derived (from eq. (14) and (94) in [4]) and coded:

$$f\left(Ri_g\right)\rightarrow f\left(Ri_f\right)=1-\frac{Ri_f}{R} \tag{6}$$

where Ri_f is flux Richardson number and R is functional dependency (constant function for model II) used for computation of stability functions. Notice that $f(Ri_g)$ has now become $f(Ri_f)$. The other SD option ($L_{TKE} \sim L_\varepsilon$) is also considered here, where L_ε is given by:

$$L_\epsilon=\frac{C_\epsilon}{v^3}\cdot\frac{\chi_3^{3/2}}{f\left(Ri_g\right)^{3/4}}\cdot l_m \tag{7}$$

However, the verification scores are worse (not shown here), which is mostly related to significant overestimation of mixing due to unlimited value of conversion coefficient in unstable stratification (Fig 1.; red curve). Also notice that mixing in stable stratification is significantly increased when compared to L_K option, thus probably leading to deterioration of verification scores.

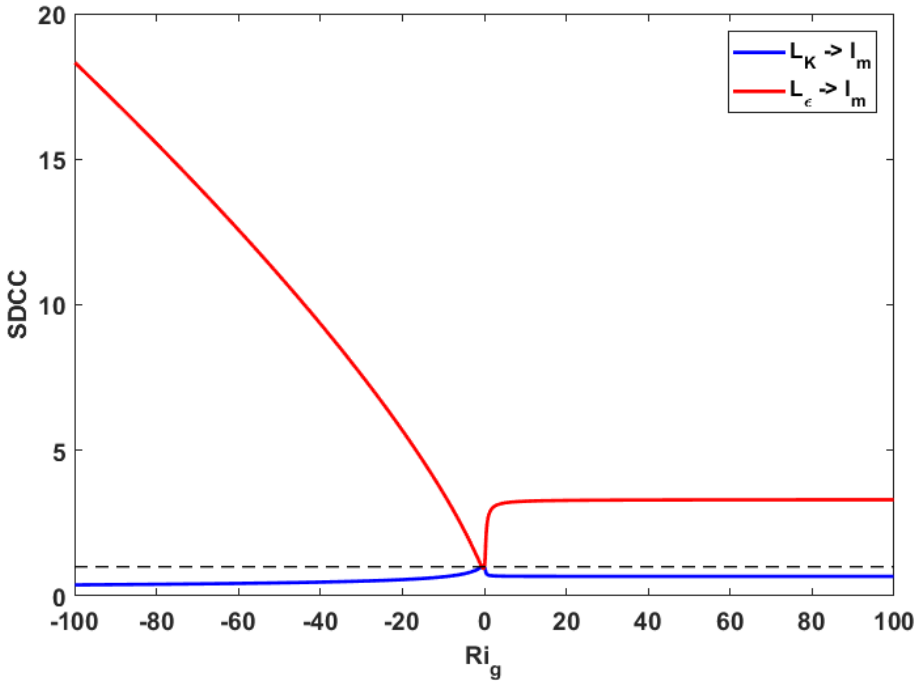

Fig 1. Stability-dependent conversion coefficient (SDCC; factor containing the ratio of $f(Ri_g)$ and χ_3, e.g. eq. (4)) plotted as a function of gradient Richardson number (Ri).

The diagnostics of averaged mixing length profiles (Fig 2.) shows that both SD BL89 options, given by (5a) or (5b) and combined with (4), lead to increase of mixing over the default option (i. e. the one where it is assumed that L_{TKE}=L and with similar averaging operator as used in Meso-NH model; check eq. (5) and (9) in [2]) which is desired feature. An increase of average mixing in most of the cases leads to an increase of average turbulence intensity (TKE; Fig 3.). However, the link between mixing length and TKE is not direct nor unambiguous, so increase of the first doesn't necessarily need to lead to increase of the second. Two SD options also increase the amplitude of mixing length's daily cycle over both the reference (l_{gc}) and default BL89 option. However, it seems that during the afternoon (e.g. 00+36 hr and 00+39 hr) they produce too strong mixing. If we go back to the basics of the method (check eq. (8a-8b) or (9a-9b) in chapter 2.4.), we may easily notice that this type of problem might appear as we close towards the neutrality. In order to confirm or refute this, we will perform the SD analysis of mixing length, i.e. we will draw a series of scatter plots (l_m vs. Ri_g) to find discrepancies between formulations or between different options within BL89 formulation (Fig 4-6.). As mostly stable upper layers would "contaminate" the results, the scatter plots will be drawn for model levels 55-87, i.e. from surface to about 2.5 km.

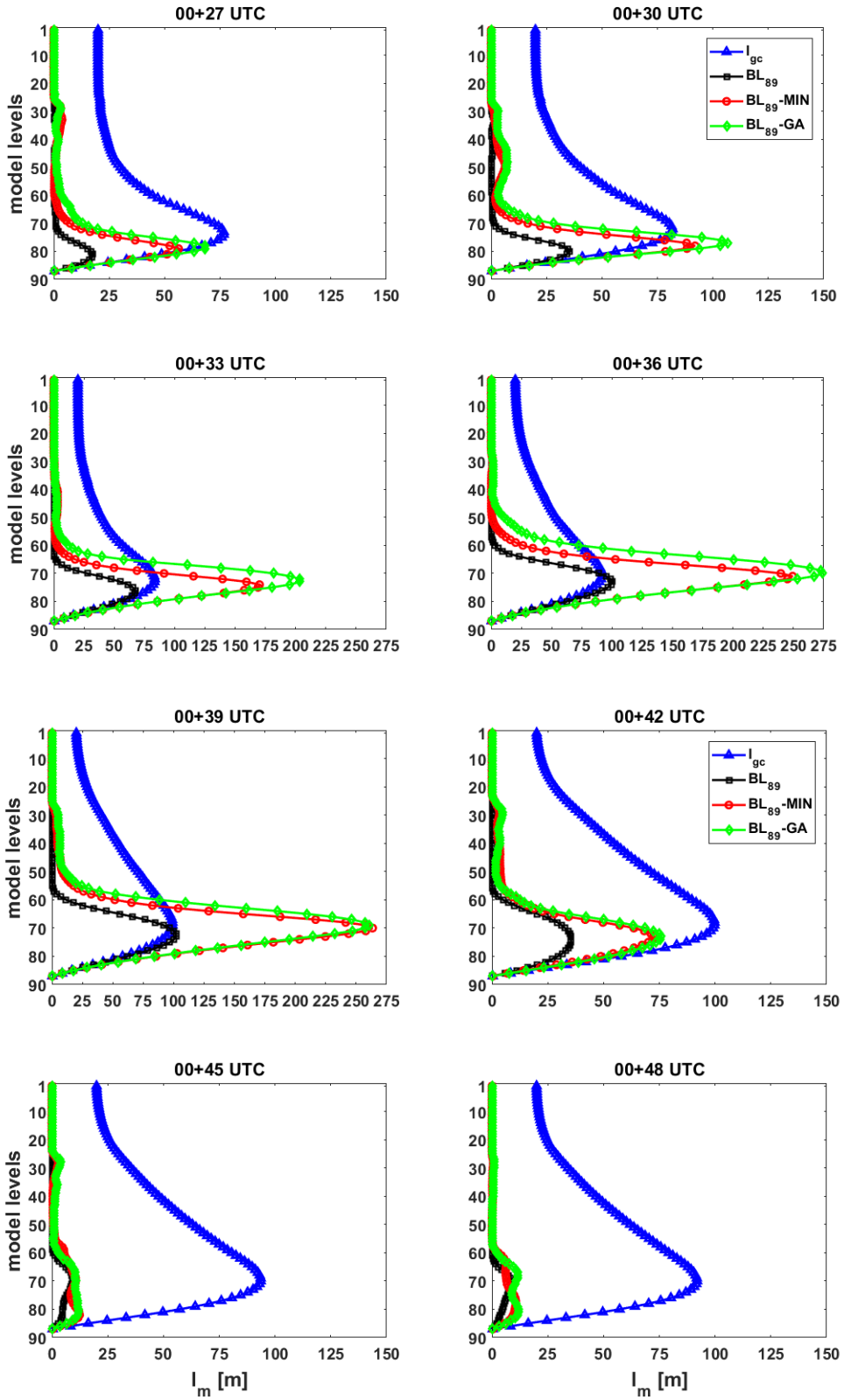

Fig 2. Averaged mixing length profile over ALADIN-CZ sub-domain (112 x 67 grid points) for Geleyn-Cedilnik formulation (l_{gc}), Bougeault-Lacarrere (1989) – BL89 with $L_{TKE} \sim L$ (as in [1]) and two stability-dependent BL89 options given by eq. (5a) - BL_{89}-MIN and (5b) - BL_{89}-GA.

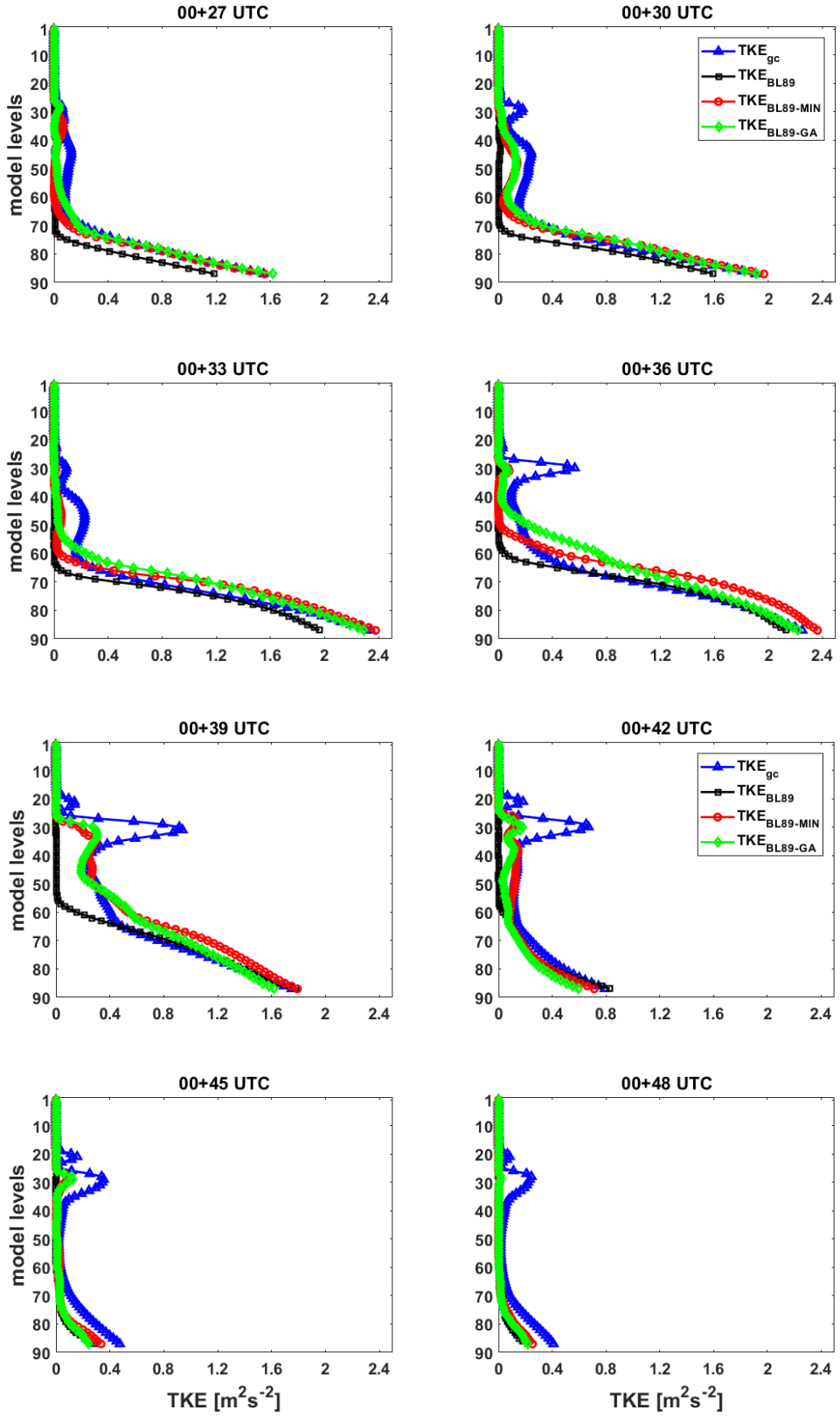

Fig 3. Averaged turbulence kinetic energy (TKE) profile over ALADIN-CZ sub-domain (112 x 67 grid points) for Geleyn-Cedilnik formulation (TKE_{gc}), default BL89 formulation (TKE_{BL89}; with $L_{TKE} \sim L$) and two stability-dependent BL89 options given by eq. (5a) ($TKE_{BL89\text{-}MIN}$) and (5b) ($TKE_{BL89\text{-}GA}$).

The stability analysis clearly shows that both SD BL89 options significantly overestimate the mixing produced by the reference near the neutrality, as well as in weakly to moderately unstable stratification (Fig 4-5.). However, in stable stratification it is the other way around. When comparing two SD options (lower panels of Fig 4-5.), one can see that they mostly differ near the neutrality, as well as in weakly to moderately stable stratification (e.g. 00+36 hr; lower panel of Fig 4.). On the other hand, sometimes the differences are rather small for any stratification (e.g. 00+39 hr; lower panel of Fig 5.). We attribute this type of behavior to L_{up}/L_{down} ratio and magnitude of L_{down} (compared to z) at particular grid point, e.g. if $L_{up}/L_{down} \sim 1$ and $L_{down} < z$, (5a) and (5b) produce similar values.

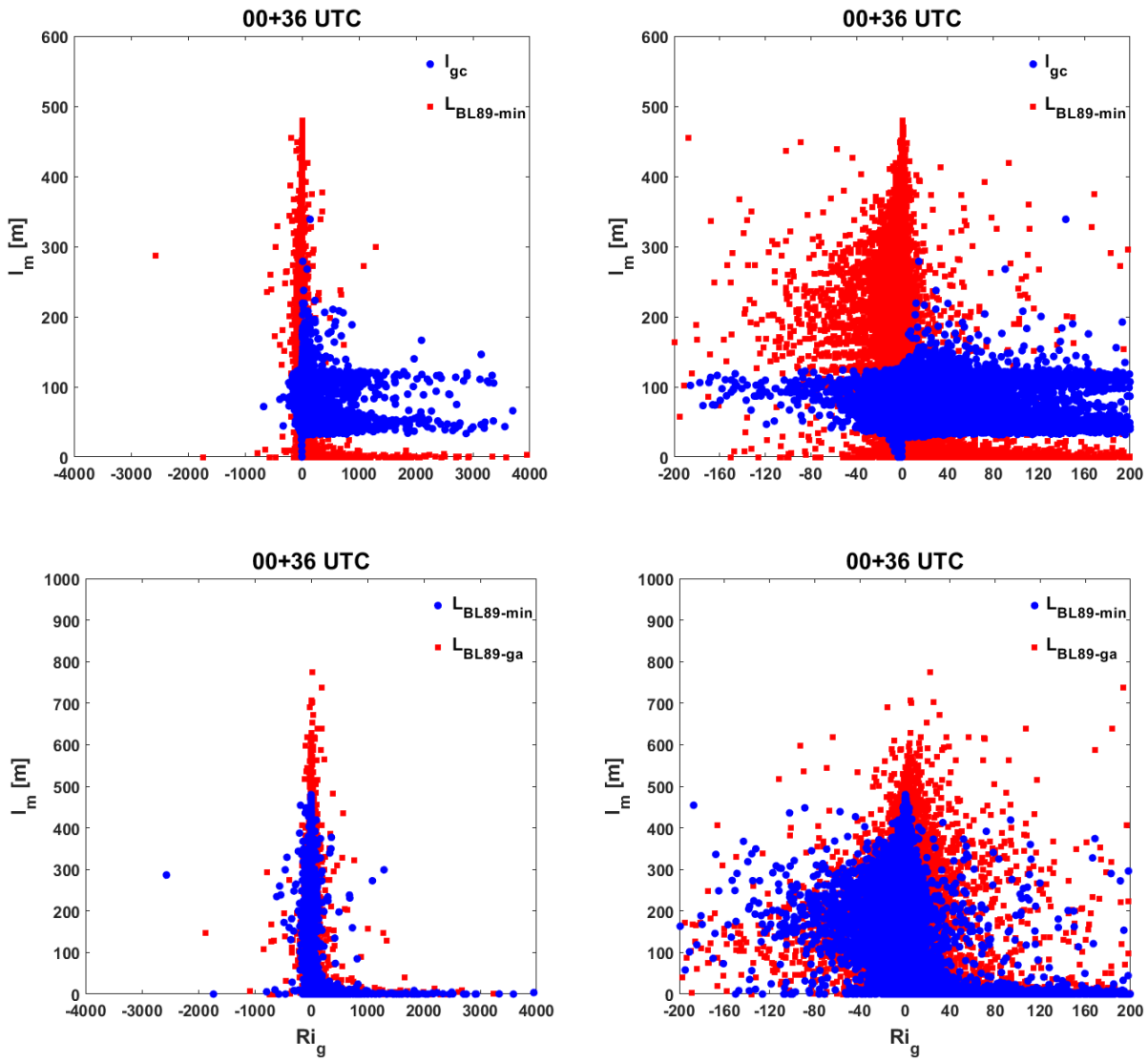

Fig 4. Scatter plot of mixing length (l_m) depending on stability (Ri_g) for: i) Geleyn-Cedilnik (l_{gc}) vs. stability-dependent Bougeault-Lacarrere (1989) - BL89 option given by eq. (5a) (upper panels) – $L_{BL89\text{-}min}$ and ii) two stability-dependent BL89 options given by eq. (5a) – $L_{BL89\text{-}min}$ and (5b) – $L_{BL89\text{-}ga}$ (lower panels)..

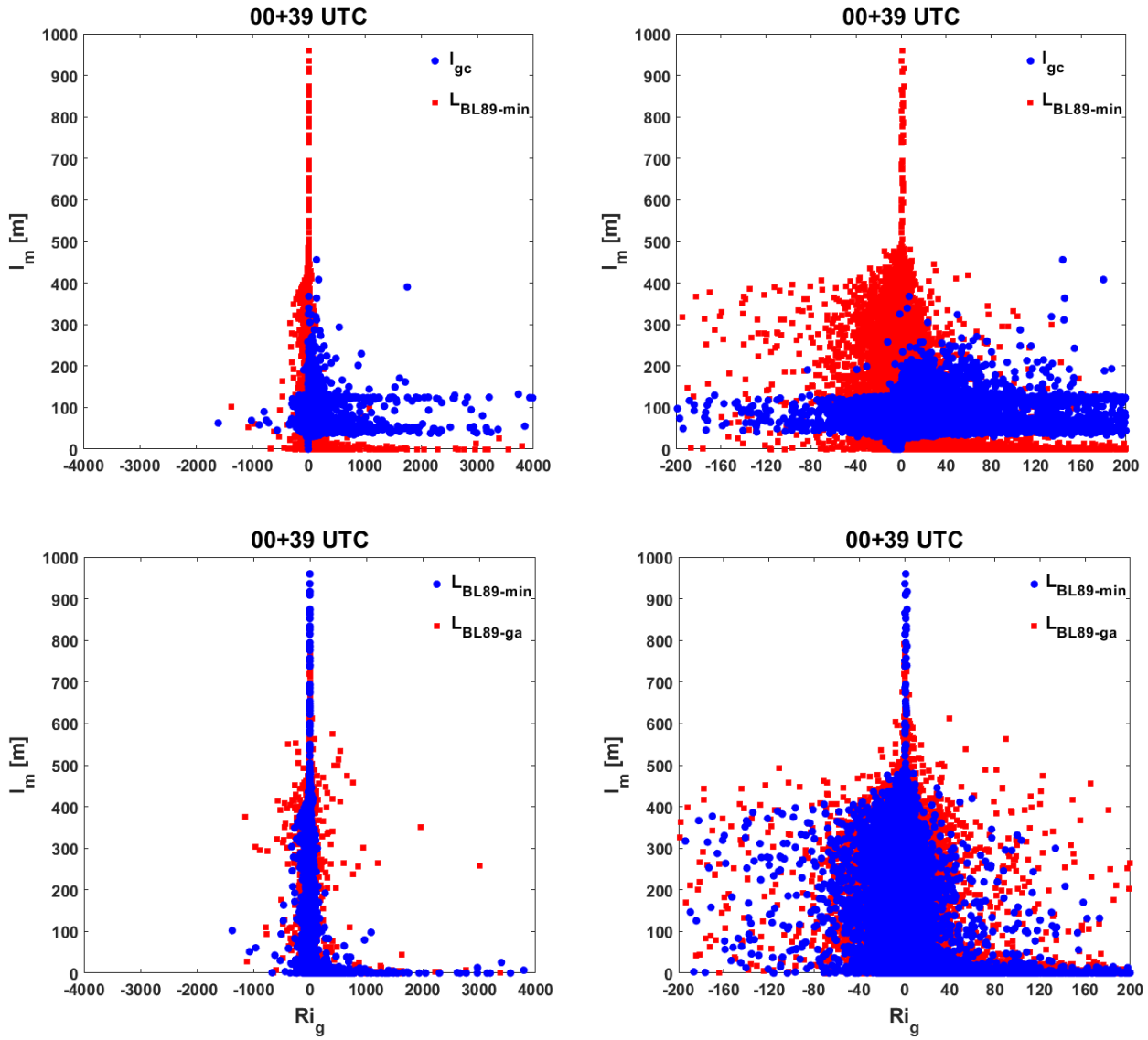

Fig 5. Scatter plot of mixing length (l_m) depending on stability (Ri_g) for: i) Geleyn-Cedilnik (l_{gc}) vs. stability-dependent Bougeault-Lacarrere (1989) - BL89 option given by eq. (5a) – $L_{BL89\text{-}min}$ (upper panels) and ii) two stability-dependent BL89 options given by eq. (5a) – $L_{BL89\text{-}min}$ and (5b) – $L_{BL89\text{-}ga}$ (lower panels).

So far we presented only the results for the summer case as there were no particular differences compared to the winter case. However, when we performed the SD analysis, one interesting feature appeared within the referent formulation (l_{gc}). Unexpectedly and contrary to the theory, the mixing in stable stratification increases with stability (Fig 6.). For the time being, there is no explanation for such a behavior. However, independent on the outcome of TKE-based formulations development, this feature has to be further revised as l_{gc} formulation is used operationally in RC-LACE countries.

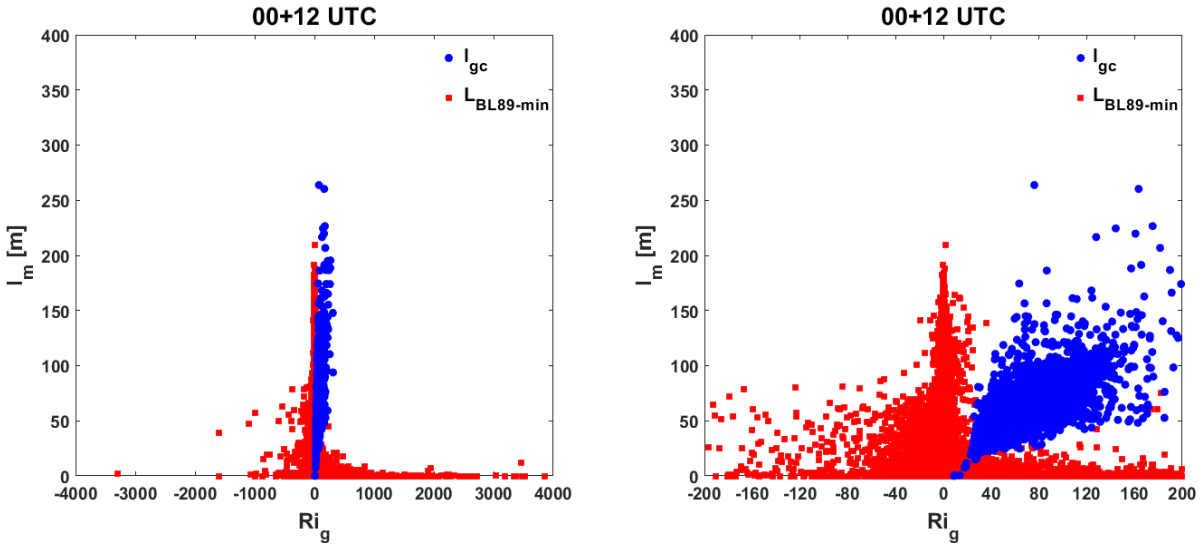

Fig 6. Scatter plot of mixing length (l_m) depending on stability (Ri_g) for Geleyn-Cedilnik (l_{gc}) vs. stability-dependent Bougeault-Lacarrere (1989) - BL89 option given by eq. (5a) at forecast lead-times +12 hr (upper panel) and +15 hr (lower panel).

Finally, we present the results of verification for chosen parameters, i.e. temperature and relative humidity. As expected, both SD BL89 options exceed the default one in terms of scores (not shown here). However, the second one (BL89-GA) was clearly more successful (not shown here). For this reason, here we present its comparison with the reference (Fig 7-9.). Near the surface SD formulations still don't show significant improvement compared to the reference (Fig 7.). However, the deficiency is currently only in BIAS, as STD and RMSE are almost the same. This probably indicates that our averaging operator is still not properly selected, but there is also at least one more problem that will be discussed in chapter 2.4.

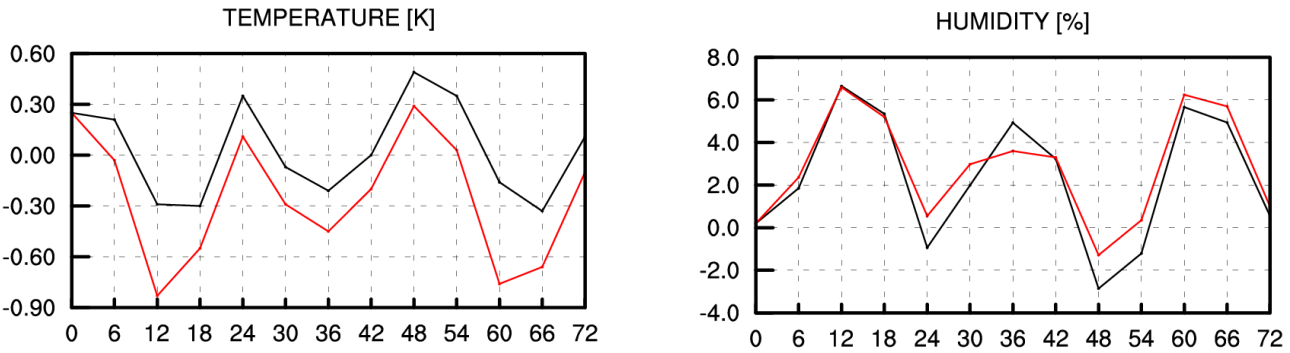

Fig 7. BIAS of temperature and relative humidity at 2 meters above surface for the reference (l_{gc}; black) and stability-dependent BL89-GA option (red), averaged over entire ALADIN-CZ domain for a summer case – 28-30.6.2017.

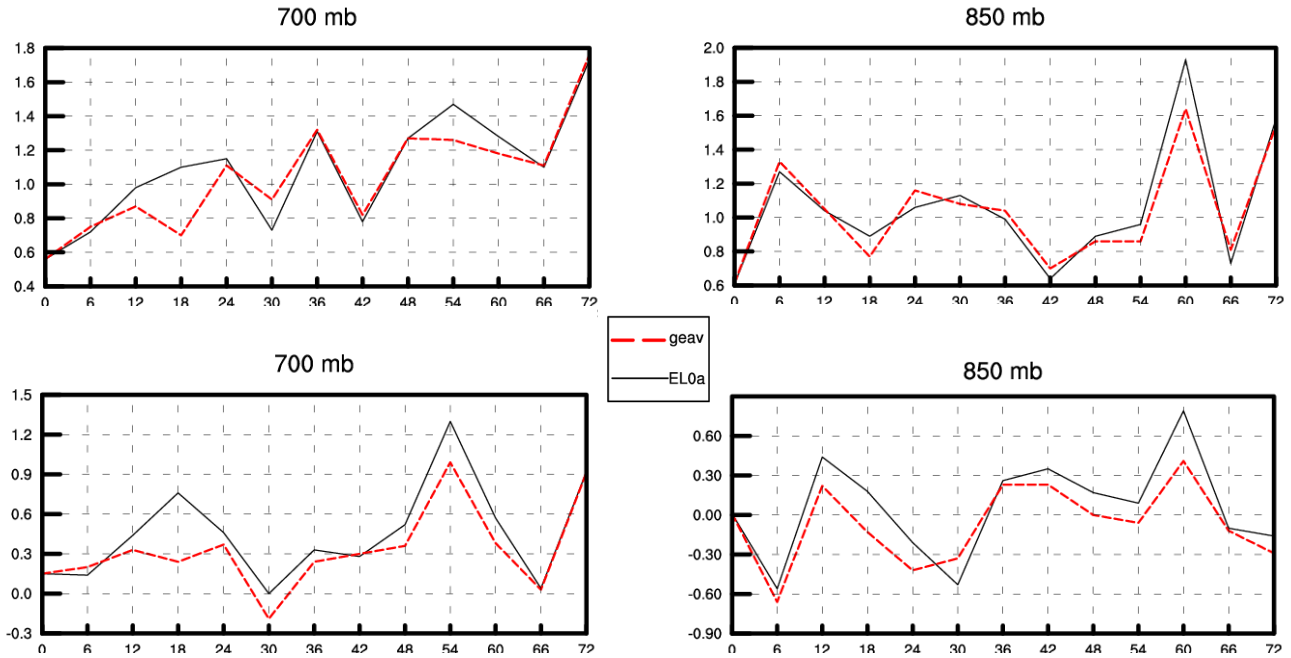

Fig 8. RMSE (upper panels) and BIAS (lower panels) of temperature for the reference (l_{gc}; EL0a) and stability-dependent BL89-GA option (geav), averaged over entire ALADIN-CZ domain for a summer case - 28-30.6.2017.

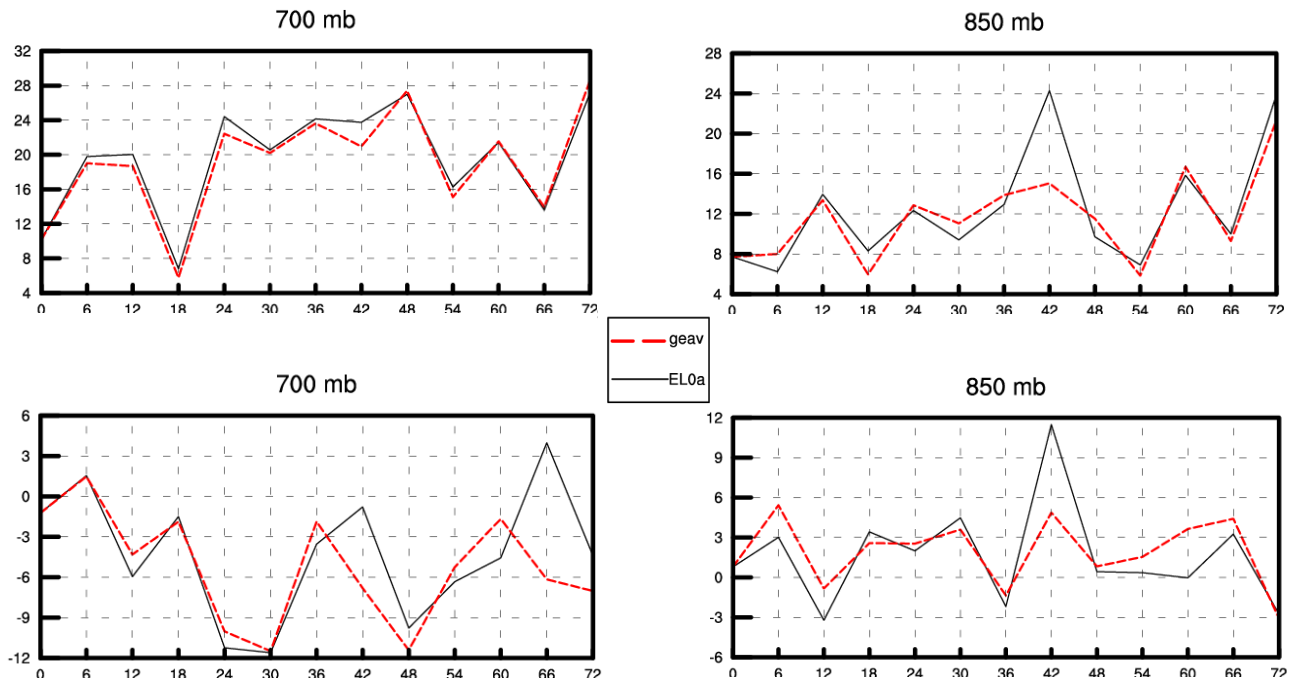

Fig 9 RMSE (upper panels) and BIAS (lower panels) of relative humidity for the reference (l_{gc}; EL0a) and stability-dependent BL89-GA option (geav), averaged over entire ALADIN-CZ domain for a summer case - 28-30.6.2017.

On the other hand, in middle and upper boundary layer the scores are at least comparable to the reference (Fig 8-9.), and sometimes even better. The later one is the case for temperature, which is slightly improved both in terms of BIAS and RMSE (Fig 8.). For the relative humidity the results are mixed (Fig 9.). Above the boundary layer, the scores for the BL89-GA option are slightly worse than for the reference (not shown here). This probably indicates that instead of imposing κz limit globally by (5b) we should find a way how to do it only locally, i.e. in the surface layer.

2.3. Experiments with TKEMULT parameter

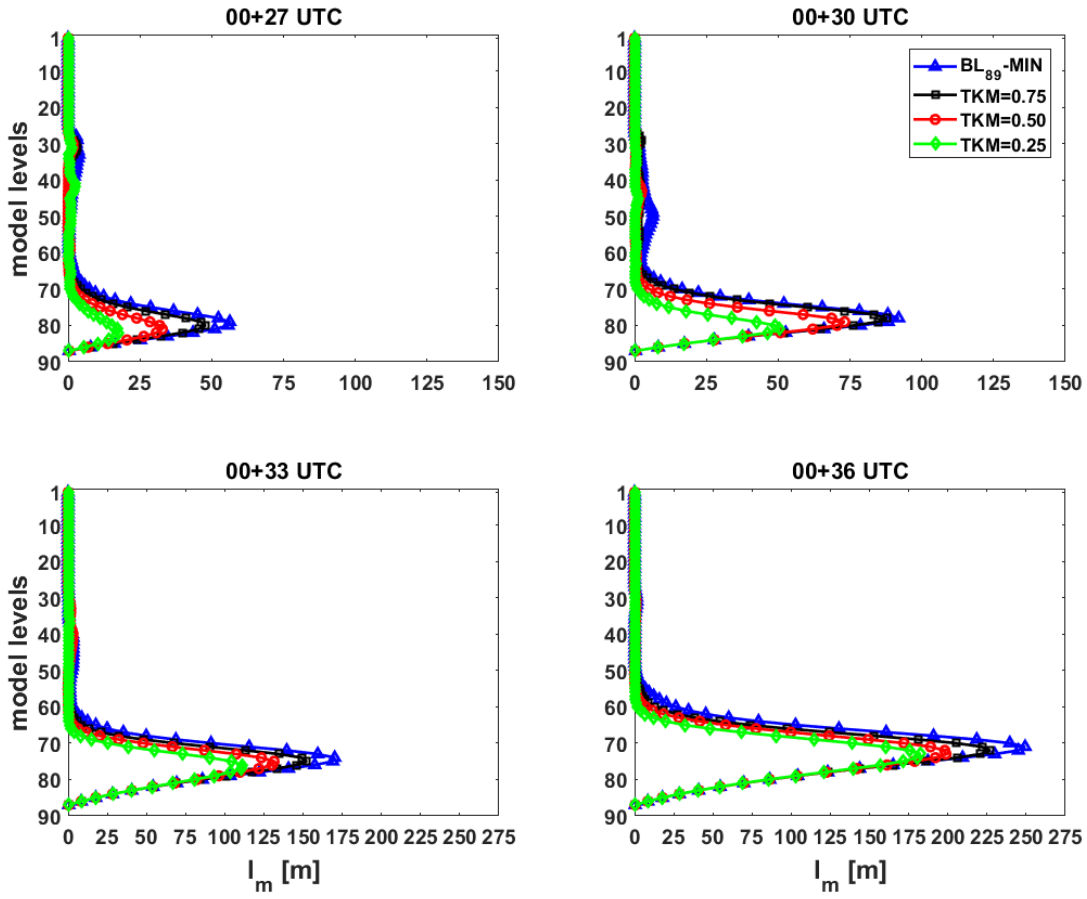

Fig 10. Averaged mixing length profile over ALADIN-CZ sub-domain (112 x 67 grid points) for Bougeault-Lacarrere (1989) – BL89 stability-dependent option (TKM=1.0) given by eq. (5a) and modifications obtained by multiplying the displacement source (TKE) with different factors. Notice a different scale on the x-axis.

TKEMULT is a namelist controlled parameter used for fine tuning of vertical displacement source term (TKE). By default TKEMULT=1, i.e. there is no modification of the right-hand side in

original BL89 equations (e.g. check eq. (1-2) and (4-5) in [6] or eq. (8a-8b) and (9a-9b) below in chapter 2.4.). As it was shown in previous experiments, both SD BL89 options lead to significant overestimation of mixing near the neutrality and in unstable stratification (over the reference – l_{gc}), while in stable stratification it is vice versa. The idea behind the TKEMULT experiments is to reduce overall mixing (i.e. to close it to the reference) by reducing the source, and hope that the greatest impact will be within the above mentioned stability range where overestimation is occurred. Further reducing of mixing in stable stratification shouldn't be a problem as it is overestimated by the reference.

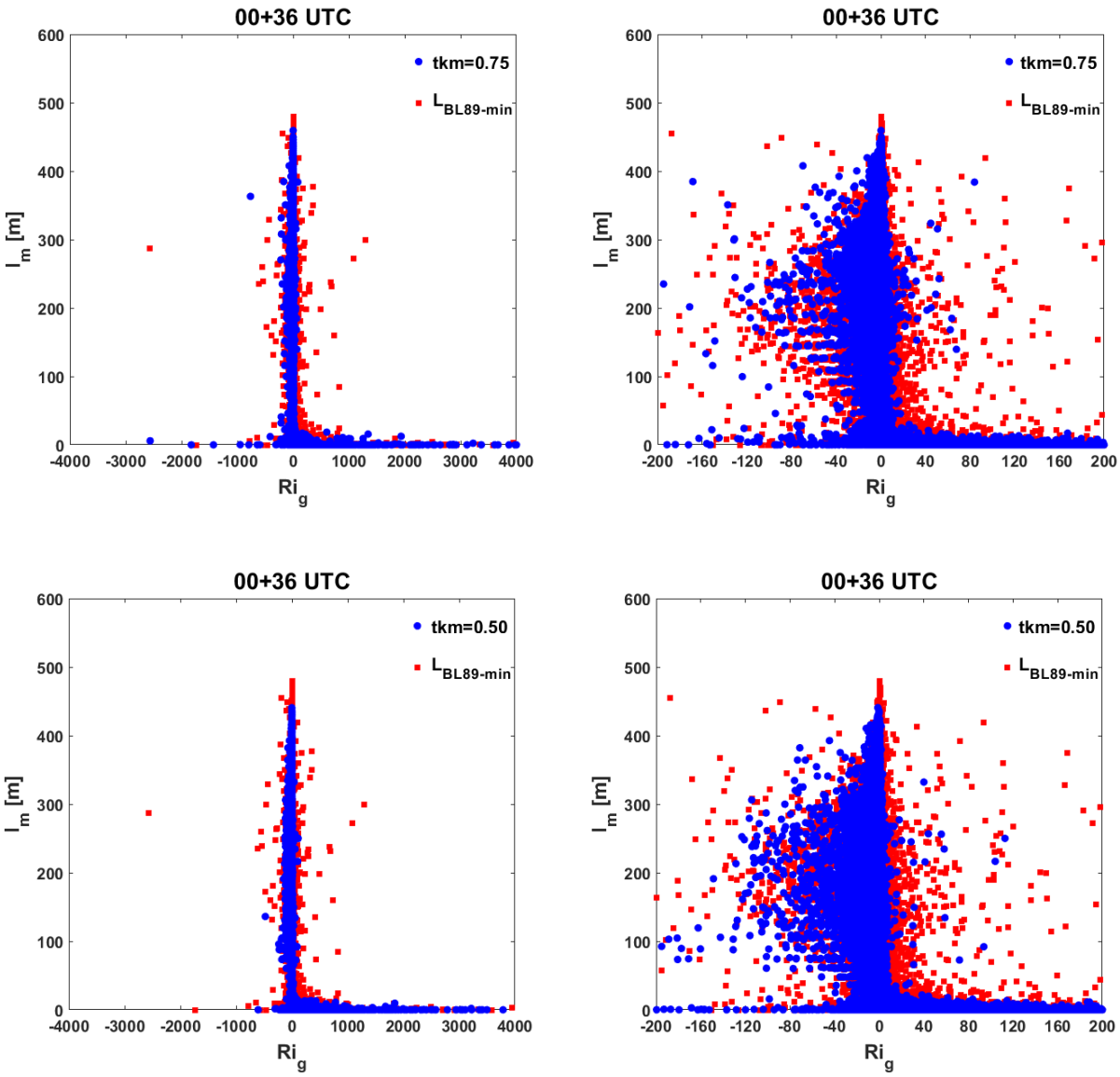

Fig 11. Scatter plot of mixing length (l_m) depending on stability (Ri_g) for stability-dependent Bougeault-Lacarrere (1989) - BL89 option given by eq. (5a) and its two modified versions: i) TKMULT=0.75 (upper panels) and ii) TKMULT=0.50 (lower panels).

We performed four experiments with TKEMULT=0.25, 0.50, 0.75 and 1.00. All experiments are performed within the BL89-MIN option, i. e. mixing length is calculated according to (5a), as a smaller of two displacement values. Averaged vertical profiles of mixing length at different forecast lead times (Fig 10.) suggest that the impact of particular TKEMULT value changes throughout the day, which is probably related to different stability regimes. For this reason we performed the SD analysis which showed that reducing of mixing is strongest in the stable stratification, but similar for both TKEMULT=0.75 and TKEMULT=0.50 (Fig 11.). Somewhat unexpectedly, the impact in the target stability region is quite small. SD analysis for TKEMULT=0.25 experiment is not even performed, as it produced very poor scores (RMSE and BIAS; not shown here). Moreover, the scores for TKEMULT=0.75 and TKEMULT=0.50 experiments are mostly worse than for TKEMULT=1.00. So, we conclude that the observed problem of overestimation of mixing near the neutrality (by BL89 SD options) and in unstable stratification needs more sophisticated way of dealing with it, e.g. by including shear effects as in [8].

2.4. Diagnostics of vertical displacement

During the process of adding the shear effects to BL89 method (according to Rodier et. al 2017.) a part of ***ACMIXELEN*** subroutine, where vertical displacements of air parcel (L_{up} and L_{down}) are computed, was checked in detail. We also checked the corresponding theoretical background given by [3] and [6]. Originally, the BL89 method is based on equations (8a) and (8b)[3], while in TOUCANS it is coded according to (9a) and (9b)[6]:

$$\int_{z}^{z+l_{up}} \frac{g}{\theta_v(z')} \cdot \left[\theta_v(z') - \theta_v(z)\right] dz' = e(z) \tag{8a}$$

$$\int_{z-l_{down}}^{z} \frac{g}{\theta_v(z')} \cdot \left[\theta_v(z) - \theta_v(z')\right] dz' = e(z) \tag{8b}$$

$$\int_{z}^{z+l_{up}} N_v^2(z'-z)\, dz' = e(z) \tag{9a}$$

$$\int_{z-l_{down}}^{z} N_v^2(z-z')\, dz' = e(z) \tag{9b}$$

where θ_v is virtual potential temperature, N_v is Brunt-Väisälä frequency, while e is turbulence kinetic energy (TKE). Overall, we identified three issues related to theory, transition from theta

((8a) and (8b)) to Brunt-Väisälä frequency approach ((9a) and (9b)) and practical implementation of the method:

- The virtual potential temperature in denominator of (8a) and (8b) is a function of z', which is not highlighted neither in [3], nor in [6]. However, this is easily checked by computing the work done against buoyancy. The overall effect is expected to be relatively small.

- Transition from (8a) and (8b) to (9a) and (9b) is only appropriate in case of special θ_v profile, i.e. equivalent to vertically constant N_v

- In practical implementation (z'-z) factor in equations (9a) and (9b) is replaced by dz (layer thickness), which can be done for the starting layer. However, higher up (if integration path covers several layers) (z'-z) is significantly higher than dz. This results in overestimation of L_{up} and L_{down} in stable stratification (smaller value of integral – longer integration path), while in unstable stratification it leads to slower accumulation of available energy (smaller value of integral – less addition to the right-hand side).

By using trapezium rule we implemented 2nd order accurate algorithm for computation of L_{up} and L_{down}, based on (8a) and (8b), i. e. assuming simpler step-wise constant integrand would lead to vertical displacement being equal to at least first layer thickness. The algorithm is implemented in full diagnostic mode within Geleyn-Cedilnik (l_{gc}) mixing length formulation. By doing so, we are able to estimate the pure impact of discretization of vertical integrals, i. e. without feedback effects due to differences in forecast evolution. We performed three simulations, wherein the first two are based on old approach by using "dry" (virtual temperature effect; BVF-dry) and moist (with phase changes effects; BVF-moist) Brunt-Väisala frequency, while the third one is based on the newly implemented theta 2nd order accuracy algorithm (theta2).

The impact of discretization method on vertical displacement of air parcel is generally significant for both L_{down} (Fig 12.) and L_{up} (Fig 13.). The differences between individual methods depend on height and direction of displacement, which is related to some of above mentioned issues, processes involved (e.g. phase changes) and displacement constraints. As a consequence of the later one, it is obvious that near the surface L_{down} is approximately equal to z (Fig 12.), i. e. displacement value is larger than the starting level height, so it is forced to that value for all three approaches. Near the level where primary maximum of L_{down} is observed (around level 70-80) theta2 method starts to differ from the other two. The reason for that is application of factor dz instead of (z-z') in (9a) and

(9b), which results in overestimation of vertical displacement as explained under the above mentioned issue number three. By entering the cloud layer, above the primary maximum of L_{down}, two Brunt- Väisälä frequency based methods start to differ. At lead-time +30 hr the highest effect of phase changes is observed, resulting in increase of L_{down} by almost an order of magnitude (compared to two "dry" methods). The differences between theta2 and BVF-dry methods, observed above the level 75, are most likely related to an approximation used in transition from (8a) and (8b) to (9a) and (9b) (above mentioned issue number two). However, the differences are also due to 2nd order accuracy algorithm applied within the theta2 method.

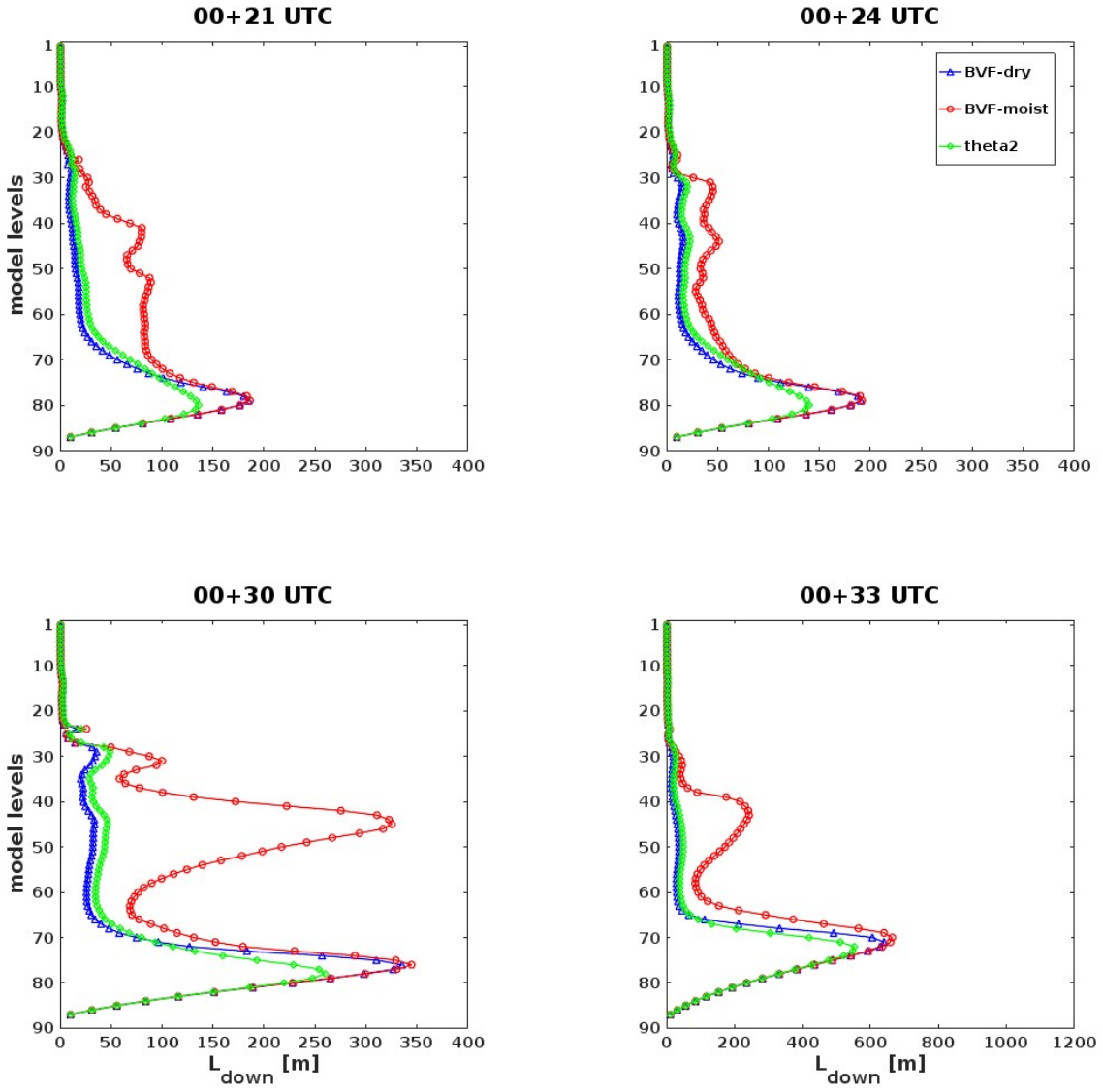

Fig 12. Comparison of L_{down} obtained by three different discretization methods using: i) "dry" Brunt-Väisälä frequency (BVF-dry), ii) moist Brunt-Väisälä frequency (BVF-moist) and iii) theta 2nd order accuracy algorithm (theta2). Notice a different scale on the x-axis.

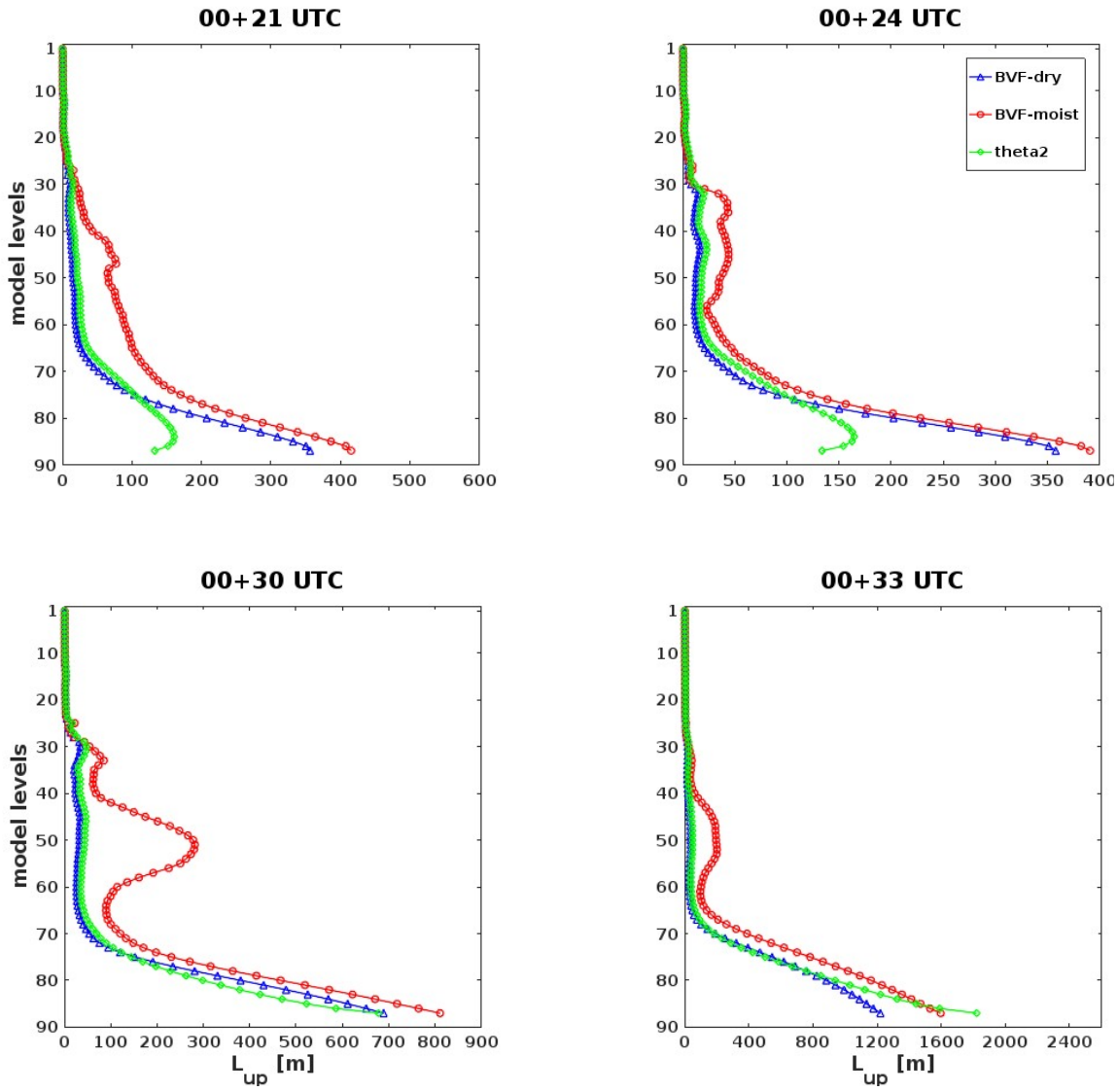

Fig 13. Comparison of L_{up} obtained by three different discretization methods using: i) "dry" Brunt-Väisälä frequency (BVF-dry), ii) moist Brunt-Väisälä frequency (BVF-moist) and iii) theta 2nd order accuracy algorithm (theta2). Notice a different scale on the x-axis.

The impact of discretization method on vertical displacement of air parcel is generally significant for both L_{down} (Fig 12.) and L_{up} (Fig 13.). The differences between the individual methods depend on height and direction of displacement, which is related to some of above mentioned issues, processes involved (e.g. phase changes) and displacement constraints. As a consequence of the later one, it is obvious that near the surface L_{down} is approximately equal to z (Fig 12.), i. e. the displacement value is larger than the starting level height, so it is forced to that value for all three approaches. Near the level where primary maximum of L_{down} is observed (around level 70-80) theta2 method starts to differ from the other two. The reason for that is application of multiplication factor dz instead of dz'

in (9a) and (9b), which results in overestimation of vertical displacement as explained under the above mentioned issue number three. By entering the cloud layer, above the primary maximum of L_{down}, two Brunt- Väisälä frequency based methods start to differ. At lead-time +30 hr the highest effect of phase changes is observed, resulting in increase of L_{down} by almost an order of magnitude (compared to two "dry" methods). The differences between theta2 and BVF-dry methods, observed above the level 75, are most likely related to an approximation used in transition from (8a) and (8b) to (9a) and (9b) (above mentioned issue number two). However, the differences are also due to 2nd order accuracy algorithm applied within the theta2 method.

Unlike L_{down}, L_{up} is not bounded. Hence, the differences between the methods are observed along the whole profile. Due to the maximum fuel available (TKE; Fig 3.), the largest upwards displacements are observed near the surface. There are also the largest differences between the theta2 and two BVF-based methods, especially during the night. The reason for this is replacing (z'-z) factor by dz in implementation of BVF-based methods, combined with large values of TKE, low spacing of model levels and nighttime stabilization of the surface layer.

It is worth noting that L_{up} obtained by theta2 method has higher near-surface amplitude of daily cycle than the one obtained by other methods. In some optimistic scenario, this might lead to more realistic daily variations of prognostic parameters. However, if mixing length is computed according to (5a), this potential benefit of theta2 method is neglected, i. e. we would always end up with $l_m=L_{down}$.

2.5. What we have learned so far (conclusion)?

The main question we are dealing with since the start of the research on this topics is to which of the length scales we should assign the output of the TKE-based mixing length formulations (L_{TKE}), i.e. to L, L_K, L_ε or l_m? By default it was assumed that $L=L_{TKE}$ which was reported to result in underestimation of mixing[4] compared to the reference (l_{gc}) and generally poor verification scores. This was also shown in [1] on a summer convection case from 2009.

After discussion with former TOUCANS developers and supervisors it was decided to go towards L_K and L_ε options, which led to SDCC between L_{TKE} and l_m (e.g. check eq. (1-2) in [2] or above eq. (4)). L_ε option was abandoned after the first test as it was unstable, or produced poor scores when simulations were performed successfully. The main reason for such a behavior is unlimitedness of corresponding conversion coefficient in unstable stratification, which leads to very high values of l_m

(Fig 1.). However, there is also a problem with overestimation of mixing in stable stratification for this SD option.

The major difference between L_K related tests in [2] and here comes from the treatment of SDCC which is now pure moist. In the meantime, we also realized that matching with Monin-Obukhov similarity theory (MOST) near the surface needs to be achieved, i.e. κz limit for l_m. For this reason we modified the proportionality coefficient between L_K and L_{TKE} (eq. (3); compare with (1-2) in [2]).

At this point we have BL89 formulation which is comparable to the reference in terms of scores, and sometimes even better. However, in terms of surface scores we are not yet successful enough. The surface problem could be resolved by implying new theta2 discretization method and by carefully selecting an averaging operator for L_{up} and L_{down} (if L_{down} is prefered by the operator, theta2 effects are almost negligible).

Finally, after additional review of literature[7] we found that:

- Above tested SD BL89 options contradict the MOST, especially in unstable stratification. If we expand SDCC from eq. (4) in Taylor series with respect to Ri_f, we end up with:

$$l_m = \left(1 - 0.18 \cdot Ri_f\right) \cdot \kappa \cdot L_{TKE} \tag{10}$$

  No matter how we calculate L_{TKE}, eq. (10) will contradict MOST due to Ri_f dependency. In stable stratification Ri_f converges to a small positive number (0.334 for model II; Fig 14.) and deviations from MOST will be rather small. On the other hand, in unstable stratification deviations will be significant as Ri_f decreases quite fast (Fig 14.) thus increasing the mixing length, e.g. for $Ri_f \approx -20$, $l_m \approx 5 \cdot \kappa \cdot L_{TKE}$ where $L_{TKE} \approx z$

- The output of TKE-based methods (L_{TKE}) shouldn't be directly assigned to any of the TKE-based scales in TOUCANS (L, L_K or L_ε) as they are all larger than z[7]. On the other hand, depending on the averaging operator for L_{up} and L_{down}, L_{TKE} can be smaller, equal or larger than z. For this reason and above explained violation of MOST, only possible option is to set $L_{TKE} \sim l_m$. Due to our selection of proportionality constant in eq. (3), for further experiments we only need to drop SDCC in eq. (4). As this coefficient is ≈ 1 near neutrality, we expect minimal differences there with $L_{TKE} \sim l_m$ approach, i.e. we will still need to find a way how to reduce mixing there.

- We are now obviously tied to selection of the scale to which L_{TKE} should be assigned. However, we are still left with two degrees of freedom: i) the choice of an averaging operator for L_{up} and L_{down} and ii) the way of including κ into l_m (until now we did it globally thus imposing κz limit everywhere). If it appears that there is insufficient mixing above the surface layer, then we will need to find a way how to include κ only locally.

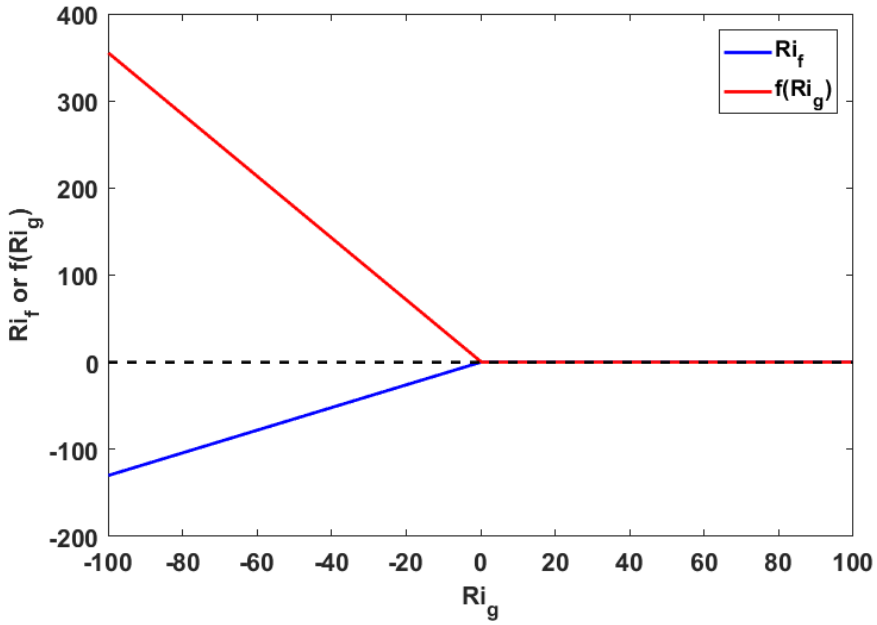

Fig 14. Richardson flux number (Ri_f) and function of Richardson number ($f(Ri_g)$) plotted as a function of gradient Richardson number (Ri_g).

3. Further work

In further work we need to:

- Compare the performance of corrected version of the BVF-dry discretization method (dz vs. (z'-z) factor) with theta2 method in full diagnostic mode

- Decide whether we need to include the effect of phase changes in computation of L_{up} and L_{down} (e.g. BVF-moist discretization)

- Select an averaging operator for L_{up} and L_{down}. If necessary, find a way how to impose κz limit only in the surface layer, i.e. without setting $l_m = \kappa \cdot L_{TKE}$, which reduces mixing globally.

- Test modified (according to above) BL89 formulation in prognostic mode and perform detailed diagnostics.

- Implement improved version of the BL89 formulation which includes shear effects (according to [8])

Acknowledgment: I would like to thank RC-LACE for funding this stay, as well as to my supervisors Ján Mašek and Radmila Brožková for support and fruitful discussions during and after the stay in Prague.

4. References

[1] Mario Hrastinski, 2016: TOUCANS - mixing length computation, RC LACE stay report, Prague, 29th February - 24th March 2016.

[2] Mario Hrastinski, 2017: Mixing length computation in TOUCANS, RC LACE stay report, Prague, 24th April - 19th May 2017.

[3] Bougeault, P. and P. Lacarrere, 1989: Parametrization of Orography-Induced Turbulence in a Mesobeta-Scale Model, *Mon. Wea. Rev.*, **117**, 1872-1890.

[4] Bastak Duran, I., 2015: TOUCANS documentation (15th July version)

[5] Deardorff, J., W., 1980: Stratocumulus-capped mixing layers derived from a three-dimensional model, *Bound.-Layer Meteorol.*, **18**, 495–527, doi:10.1007/BF00119502.

[6] Vana, F., I. Bastak Duran, and J.-F. Geleyn, 2011: Turbulence length scale formulated as a function of moist Brunt-Väisälä frequency. *WGNE Blue Book*, chap. 4, 9-10.

[7] Redelsperger, J.-L., F. Mahé, and P. Carlotti, 2001: A simple and general subgrid model suitable both for surface layer and free-stream turbulence, *Bound.-Layer Meteor.*, **101**, 375–408, doi:10.1023/A:1019206001292.

[8] Rodier, Q., Masson, V., Couvreux, F., and Paci, A., 2017: Evaluation of a Buoyancy and Shear Based Mixing Length for a Turbulence Scheme. *Front. Earth Sci*. 5:65. doi:10.3389/feart.2017.00065